AIP Advances

Investigation of various magnetic features of spinel type cobalt ferrite ($CoFe_2O_4$) nanoparticles tuned by annealing temperature

Cite as: AIP Advances **8**, 105124 (2018); https://doi.org/10.1063/1.5040890
Submitted: 22 May 2018 . Accepted: 10 October 2018 . Published Online: 22 October 2018

Probal Roy, S. Manjura Hoque, S. I. Liba, and Shamima Choudhury

Investigation of various magnetic features of spinel type cobalt ferrite ($CoFe_2O_4$) nanoparticles tuned by annealing temperature

Probal Roy,[1,a] S. Manjura Hoque,[2] S. I. Liba,[2] and Shamima Choudhury[3]
[1]*Department of Physics, Khulna University of Engineering & Technology, Khulna 9203, Bangladesh*
[2]*Materials Science Division, Bangladesh Atomic Energy Commission, Dhaka 1000, Bangladesh*
[3]*Department of Physics, University of Dhaka 1000, Bangladesh*

(Received 22 May 2018; accepted 10 October 2018; published online 22 October 2018)

Cobalt ferrite ($CoFe_2O_4$) nanoparticles synthesized by chemical co-precipitation method were studied to see the effect of annealing temperatures on the structural parameters and magnetic properties of the sample. X-ray powder diffraction (XRD), transmission electron microscope (TEM) and SAD pattern demonstrated that single face (fcc) spinel structure of $CoFe_2O_4$ has been formed showing particles in completely crystalline state which was further confirmed by the lattice parameter and the unmixed hkl values. The particle size is in the range of about 5-10 nm depending on the annealing temperature from 200°C to 400°C. The grain growth occurred monotonically with the increase of annealing temperature. The magnetic properties demonstrated a strong dependence on particle size. The saturation magnetization M_s, remanent ratio M_r/M_s and coercivity H_c increased with the increase of particle size. The hysteresis curves for samples of different grain size showed the ferrimagnetic behavior which is completely analogous to the slow relaxation sextet peaks of Mössbauer spectroscopy. Other parameters such as chemical shift, quadruple splitting and hyperfine field and site occupancy of Fe^{3+} were determined by Mössbauer spectroscopy. Ferrimagnetic to superparamagnetic transition temperature known as blocking temperature T_B was determined from the temperature dependent magnetization curves. With the increase of grain size, Blocking temperature also increases. Maximum entropy changes due to magnetic phase transition were also observed for mentioned annealing temperatures in the context of Magnetocaloric effect. https://doi.org/10.1063/1.5040890

I. INTRODUCTION

In recent days, nanocrystalline ferrites become a subject of fascination because of their overwhelming application in human life as well as research areas. Iron-oxide nanoparticles have been used as an important specimen in the field of research and practical life on account of their unusual physical, electronic and magnetic properties compared to their bulk counterparts. However, with the reduction of particle size into nanoscale, some of these properties change drastically.[1–5] Complex relationship between nanostructural features and the macroscopic magnetic properties are not same for all combinations. To know the applications of a combination of ferrite, it is mandatory to inspect this relationship properly.[6]

Nanoparticles are important scientific tools that have been and are being explored in various biotechnological, pharmacological, industrial and technological uses. In biomedical fields, nanocrystalline ferrites have outstanding applications like magnetically guided drug delivery, magnetic

[a]Email: probal.phy@gmail.com

resonance imaging, hyperthermia etc where the conventional drugs may not work.[7,8] Moreover, in the field of environmentally friendly magnetic refrigeration technology, ferrite nanoparticles are extensively used as a substitution of rare earth materials due to their reasonable cost and easy procurement. These applications of ferrite are influenced by the physical and chemical properties of the materials including microstructure, combination, particle size etc. These properties are dependent on some factors such as synthesis process, concentration, heating and cooling condition, annealing temperature, annealing time etc.[9] Small amount of change in any of these factor may consequence to drastic change in properties of ferrites.

A remarkable example is that of, cobalt ferrite ($CoFe_2O_4$) which has drawn attention due to its exquisite physical and chemical stability, reasonable saturation magnetization, high remanence and high magneto-crystalline anisotropy.[2,10] The crystal structure of $CoFe_2O_4$ is inverse spinel type structure where oxygen atoms constitute a face center cubic (fcc) lattice. In this regard, divalent Co^{2+} ions are shifted to octahedral "B" sites and trivalent Fe^{3+} ions are occupied by both tetrahedral "A" and octahedral "B" sublattice sites.[11,12] Ferrimagnetism are witnessed in cobalt ferrite due to unequal antiferromagnetic A-B superexchange interaction by the collaboration of the magnetic dipole moments.[13]

Now-a-days, Global warming is a crucial threat for world's environment and ecosystem. One of the principal reasons of global warming is the inflation of ozone depleting chemicals and greenhouse gases such as Chloflurocarbons (CFC), Hydrochloflurocarbons, Hydroflurocarbons etc. These environmentally toxic elements have been used mostly in our refrigeration system. In this concern, magnetic refrigeration is a newly highly efficient and environmental friendly refrigeration system that does not use green house and CFC gas. The basis of magnetic refrigeration is known as magnetocaloric effect. The magnetocaloric effect is a "Magneto Thermodynamic" phenomenon that is acquainted with the heating and cooling of magnetic materials due to the application of the external magnetic field. Typically, a magnetic material with a noticeable magnetocaloric effect (MCE) will rise in temperature upon application of an applied field and will lower in temperature upon relaxation of the field. The mechanism of the change in temperature and the change in entropy arises from the manipulation of the magnetic moments in the materials. If the system is kept under isothermal conditions and constant pressure, the total entropy will decrease when a field is applied and increases when the field is removed. If the system is kept under adiabatic conditions and constant pressure, the total entropy remains constant. In this regard, the temperature increases when the field is applied and decreases when the field is removed.[14–16]

The aim of this study is to synthesis $CoFe_2O_4$ nanoparticles by chemical co-precipitation method and to observe the effect of annealing temperature on the structural properties and to characterize various magnetic properties including hysteresis loop, Saturation magnetization, remanent ratio, coercivity, Mössbauer analysis, superparamagnetic behavior at different annealing temperatures and magnetocaloric effect observation in the vicinity of superparamagnetic blocking temperature.

II. EXPERIMENTAL SETUP

To synthesize $CoFe_2O_4$ nanoparticles, analytical grade powder of $CoCl_2.6H_2O$ salt and $FeCl_3$ were mixed in the molar ratio of 1: 2 and 8M of NaOH solution was added under continuous stirring. NaOH was added to control the pH of the solution. The mixture was heated to 80°C for 1h. Then it was followed by centrifugation operation at 13500 rpm for 20 min and was washed by filtration. The centrifugation and filtration were done for 10 times to remove NaOH from the precipitate. Then the final precipitate was dried at 80°C for 72h. After drying, pellets were prepared from the as-dried powder. Then the pellets of the samples were annealed in the temperatures 200°C and 400°C.[17]

For structural characterization of $CoFe_2O_4$ nanoparticles, X-ray diffraction patterns for the samples in different annealed conditions were studied that were recorded on a Philips X'Pert Pro powder X-ray diffractometer (PW 3040) by using Cu-K_α (λ= 1.54 Å) radiation. For all the measurements of $CoFe_2O_4$, powder specimens of about 15mg were exposed to Cu – K_α radiation with a primary beam power of 40kV and 30mA with a sampling pitch of 0.02° and time for each step data collection was 1 second. TEM bright field (BF) image and SAD pattern was acquired for further structural characterization of as-dried powder by F30 transmission electron microscopy (TEM) technique.

The image was acquired by drop drying the diluted nanoparticle solution on the Cu grid. Hysteresis curves, temperature dependent magnetization curves and isothermal magnetization curves were carried out by Vibration sample magnetometer (Model: EV-9, Microsence LLC, USA). Moreover, magnetic phase identification and magnetic ordering were studied by Mössbauer spectrometer (SEE Co. Model VT 400).

III. RESULTS AND DISCUSSION

The X-ray diffraction patterns for $CoFe_2O_4$ nanoparticles for as-dried particles and annealed at 200°C and 400°C are presented in the Fig. 1. The comparison between the XRD pattern and the standard data (JCPDS PDF card no. 22-1086) confirms the formation of $CoFe_2O_4$ nanoparticles. The single phase cubic spinel structure (fcc) with reflections from planes of (220), (311), (400), (422), (511) and (440) was identified.[18,19] The broadenings of the XRD line indicated that the $CoFe_2O_4$ nanoparticles was of nano dimension. Whereas annealing brings about increase in grain growth giving rise to narrow and sharp well defined peaks. The crystallite size of all the heat treated samples of $CoFe_2O_4$ nanoparticles was determined using Scherrer's formula.[10]

$$D = \frac{K\lambda}{\beta cos\theta} \tag{1}$$

The crystallite size for the $CoFe_2O_4$ nanoparticles has been demonstrated in the range about 5-10 nm for the samples in as-dried condition and annealed at 200°C and 400°C. It can be observed that with the increase of annealing temperature, the grain growth occurred monotonically.

The lattice parameter 'a' of the samples with different annealing conditions were determined by using following formula,

$$a = d\sqrt{h^2 + k^2 + l^2} \tag{2}$$

The variations of crystallite size and lattice parameter with respect to temperature are shown in Table I. The difference in the values of lattice parameter of the as-dried samples and the annealed samples at different temperatures ranging from 200°C to 400°C is a result of the change in surface to volume ratio. This is because the lattice parameter of the spinel lattice depends on the complex interplay between the size of the ions and their distribution.[20]

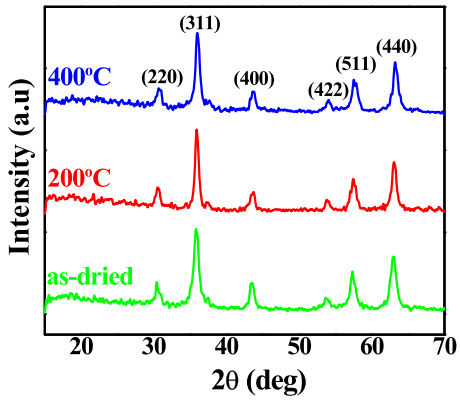

FIG. 1. X-ray diffraction patterns of $CoFe_2O_4$ nanoparticles for as-dried samples and for T_a= 200°C and 400°C.

TABLE I. The Lattice parameters and Crystallite sizes of $CoFe_2O_4$ at different annealing temperatures.

Annealing Temperature (T_a) °C	Lattice Parameter (a) Å	Grain Size (D) nm
as-dried	8.312	5.21
200	8.345	6.40
400	8.586	9.29

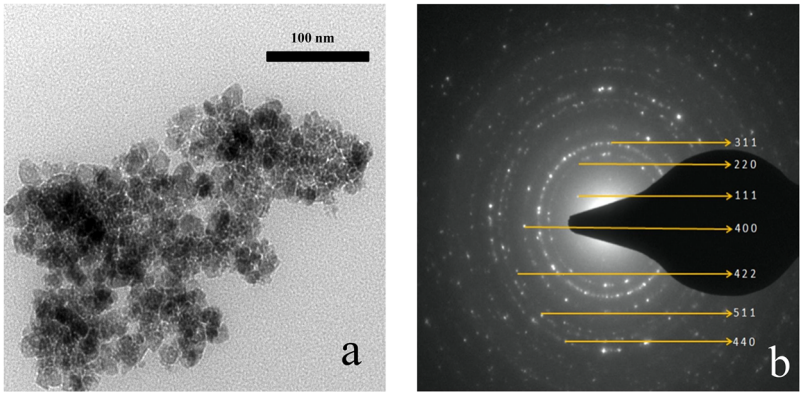

FIG. 2. (a) TEM bright field image of $CoFe_2O_4$ nanoparticles annealed at 200°C. (b) Selected Area Diffraction (SAD) pattern for $CoFe_2O_4$ nanoparticles.

To observe the morphological properties i.e. physical size and shape of the $CoFe_2O_4$ nanoparticle TEM (Transmission Electron Microscope) bright field image for the sample annealed at 200°C is presented in Fig. 2(a). In the TEM image most of the particles appear spherical in shape. Particle size of $CoFe_2O_4$ that is annealed at 200°C by XRD seems to be in fair agreement with the grain size as observed from the TEM bright field image. The inter-planar spacing obtained from SAD (Selected Area Diffraction) patterns is shown in Fig. 2(b). SAD patterns were induced by comparing the miller indices with the standard pattern.

Magnetization as a function of the applied magnetic field up to 15 kOe for the samples in the as-dried condition and in different annealed conditions ranging from 200°C to 400°C are shown in Fig. 3(a), (b), (c) and (d). Various magnetic parameters such as coercivity (H_c), saturation magnetization (M_s) and remanent magnetization (M_r) were measured from the Hysteresis loops given in Table II.

The remanent ratio M_r/M_s was found to increase with increasing of annealing temperature. Basically, the magnetization is the function of annealing temperature as well as particle size.

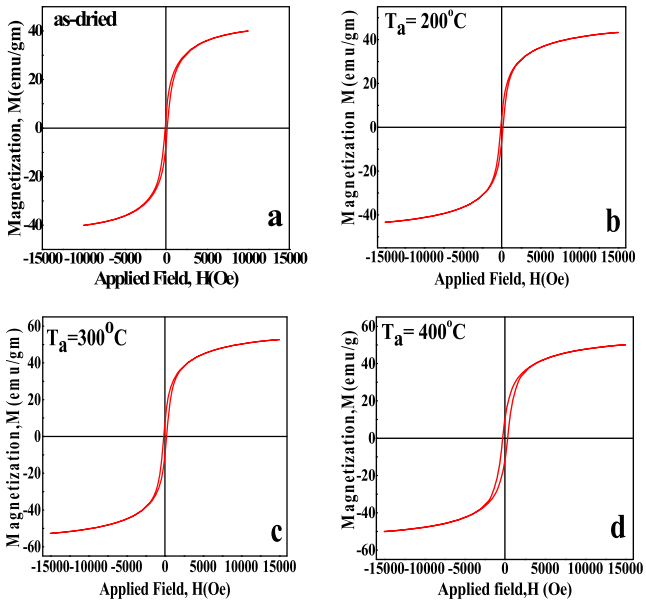

FIG. 3. (a) Hysterisis loops of $CoFe_2O_4$ nanoparticles for as-dried samples. (b) Hysterisis loops of $CoFe_2O_4$ nanoparticles for T_a= 200°C. (c) Hysterisis loops of $CoFe_2O_4$ nanoparticles for T_a= 300°C. (d) Hysterisis loops of $CoFe_2O_4$ nanoparticles for T_a= 400°C.

TABLE II. Maximum magnetization (M_{max}), Remanent magnetization (M_r) and Coercive field (H_c) after annealing at different temperatures.

Annealing Temperature (T_a) ^oC	Saturation Magnetization, M_s emu/gm	Remanent Magnetization, M_r emu/gm	M_r/M_s	Coercive field, H_c Oersted
as-dried	40.073	5.432	0.135	120.369
200	43.295	5.531	0.127	139.843
300	52.687	8.793	0.167	184.624
400	50.051	10.551	0.210	302.897

For nanoparticles the smaller the particle size, the greater the surface to volume ratio. For this reason, with decreasing nanoparticle size, more atoms are captured on the surface of the nanoparticle rather than core. So, for smaller nanoparticles, the value of normalized magnetization is small because of the greater surface disorder than bigger nanoparticles. The magnetization also rises by the increase of annealing temperature due to the reduction of the surface disorder.[21,22]

The coercivity H_c increases with the increasing of annealing temperature form the as-dried conditions i.e. with the increasing of grain size. It has been observed that, for nanoparticles, coercivity decreases with the rise of the particle size which can be expressed as $H_c \sim 1/d$, where d is the diameter of the particle. With the decrease of particle size, the role of surface in determining the anisotropy i.e., anisotropy energy increases and hence coercivity increases.[23,24] Present study shows that coercivity increases with the increase of grain size. So, the inverse relation of grain size dependent of coercivity is clearly observed, that is the break-down of conventional size law that is common for conventional bulk materials.

To estimate the distribution of the iron (Fe^{3+}) in the ferrite spinel for the different annealing temperatures, ^{57}Fe-Mössbauer spectra were recorded. Fig. 4 shows the Mössbauer spectra for as-dried samples and for two annealing temperatures, T_a= 200°C and 400°C at room temperatures. Spectral fits were performed assuming Lorentzian absorption line shapes using the Mössbauer spectral fitting

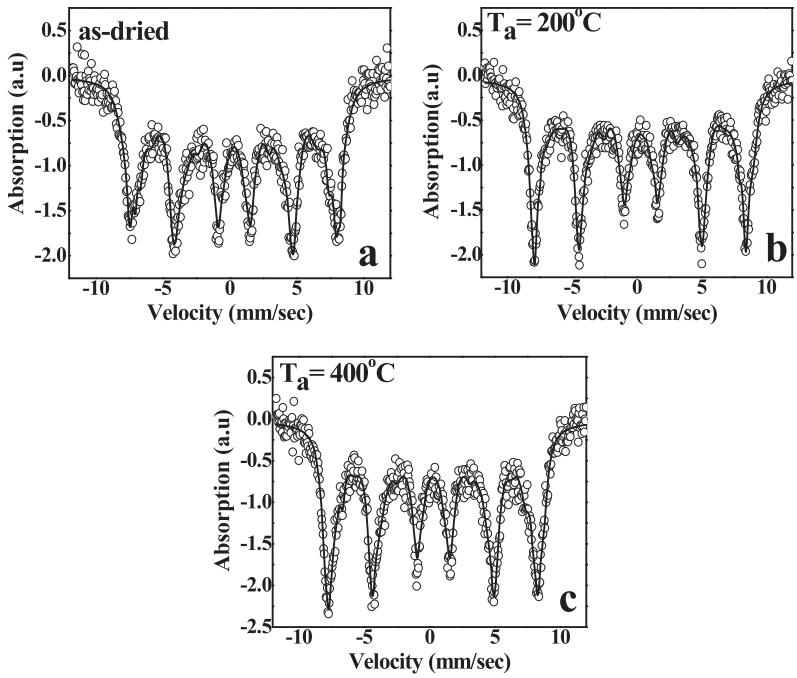

FIG. 4. (a) Mössbauer spectra of $CoFe_2O_4$ nanoparticle for as-dried samples at room temperatures. (b) Mössbauer spectra of $CoFe_2O_4$ nanoparticle for T_a= 200°C at room temperatures. (c) Mössbauer spectra of $CoFe_2O_4$ nanoparticle for T_a= 400°C at room temperatures.

TABLE III. Hyperfine parameters of Mössbauer spectroscopy at room temperature without any applied field.

Annealing Temp ^{o}C And χ^2	Site Occupancy	Chemical Shift (δ) mm/sec	Quadrupole splitting (dE_q) mm/sec	Hyperfine field (H_{int}) KG	Rel. Area (%)
as-dried	B	0.303	0.0237	-463.373	53.5
χ^2 = 1.606	A	0.334	0.116	-407.325	46.5
200	A	0.252	0.235	-400.000	35
χ^2 = 1.286	B	0.200	0.178	-471.496	65
400	A	0.271	0.305	-418.178	32.5
χ^2 = 1.428	B	0.283	0.0452	-481.693	67.5

software WMOSS 4R which includes also the slow relaxation. It can also be observed from the figures that the spectra exhibits sextet pattern that is the characteristics of slow relaxation which demonstrates that the material is in the ferrimagnetic state.[25–28]

An acceptable data fitting was obtained when the A and B-site pattern is assumed to be a superposition of more than one sextet. Consequently, the statistical distribution of Co^{2+} ions at the A-site will result from the distribution of Fe^{3+} ions in the both A-site and B-site. The various electronic and magnetic parameters such as chemical shift, quadruple splitting, hyperfine field and relative area are presented in Table III as obtained from the Mössbauer spectra. The χ^2 (goodness of fitting) values are also reported in the Table III. Based on the relative area of each species cation distribution has been estimated. It is found from the literature that, the outer subspecies represent octahedral sub site and inner subspecies represent tetrahedral subsites. It has also been assumed that the iron species exist only in trivalent form. The higher values of quadruple splitting and lower values of isomer shift and are marked in the tetrahedral position and the lower values of quadruple splitting and higher values of isomer shift marked in the octahedral position of iron groups.[29]

The occupancy of Fe^{3+} ions in the site A and site B are shown in Table III for different annealing temperatures. The corresponding Isomer shift, Quadrupole splitting and hyperfine fields provides the probable cation distribution. For as-dried samples, 53.5% of the Fe^{3+} are occupied by B-site and 46.5% of Fe^{3+} are altered to the A-site. For T_a= 200°C, 65% of the Fe^{3+} are occupied by B-site and 35% of Fe^{3+} are shifted to the A-site. For T_a = 400°C, 67.5% of the Fe^{3+} are occupied by B-site and 32.5% of Fe^{3+} are shifted to A-site.

Temperature dependent magnetization (M-T curve) has been analyzed for the as-dried $CoFe_2O_4$ nanoparticle samples and the samples annealed at 200°C and 400°C in Fig. 5(a). Blocking temperature (T_B) can be found which indicates the superparamagnetic to ferrimagnetic transition of the samples. Below blocking temperature, the specimen exhibits ferrimagnetic nature and above it shows superparamagnetic behavior.[30] For ferrimagnetic materials, the internal energy on the direction of spontaneous magnetization is related to magnetic anisotropy. In the single domain uniaxial nanoparticles, spontaneous magnetization is produced when the collective magnetic moments tend to align along certain preferred crystallographic direction. Collective magnetic moments form and fluctuate

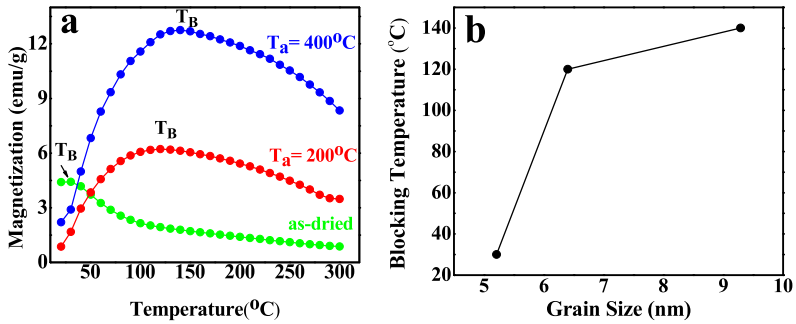

FIG. 5. (a) Temperature dependent magnetization (M-T) curves of $CoFe_2O_4$ nanoparticles for as-dried samples, T_a= 200°C and T_a= 400°C. (b) Change of Blocking temperature with respect to Grain size.

together due to interaction between moments within the particles. If thermal energy is high enough, the collective magnetic moments flip their direction many times and will no longer stay in the easy direction; the anisotropy energy is overcome by the thermal energy.[27] Superparamagnetism occurs when the magnetocrystalline anisotropy energy is much less than that required to reorient (anti-align) the individual spins; as for the volume size, it is also much less than thermal energy per unit volume. For fine magnetic particles, the actual magnetic behavior depends on the value of the measuring time (τ_m) with respect to the relaxation time (τ) associated with the overcoming of the energy barrier. The relaxation time for a magnetic moment changes with varying temperature. In superparamagnetic materials at $T > T_B$, the direction of collectively coupled magnetic moments alter for several times on account of thermal energy, which is familiar as superparamagnetic state. In this state, the relaxation time is much shorter than measured time. At certain temperature $T = T_B$, the relaxation time of the moments is equal to τ_m and collective moments will not flip any longer and a net magnetization could be observed. In this regard, the relaxation time is much longer than the measured time, so the collective magnetic moments are fixed in one direction causing an increase in the net magnetization which consequences to a blocked state.[31,32] If $T < T_B$, the magnetocrystalline energy is higher enough rather than thermal energy, so that magnetic moment of each particle lies along the easy axis, i.e., the directions are energetically degenerate and separated by an energy barrier. This state is known as ferrimagnetic state.[31]

The blocking temperatures for as-dried and the samples annealed at the temperatures of 200°C and 400°C were obtained as 30°C, 120°C and 140°C respectively. It is noticeable that, the field applied for as-dried $CoFe_2O_4$ and the samples annealed at 200°C and 400°C are 60 Oe, 160 Oe and 320 Oe respectively. It can be seen from Fig. 5(b) that, blocking temperature increases with the increase of grain size. This indicates that for the case of the nanostructured samples, the blocking effect is present and becomes dominant as the grain size is reduced. The increase in T_B is linked to the increase of Co^{2+} ions in the octahedral sites. Besides particle size, the blocking temperature can also be influenced by several intrinsic factors, which mainly include magnetocrystalline surface and shape anisotropy and extrinsic factors, generally related to interactions between particles.[30]

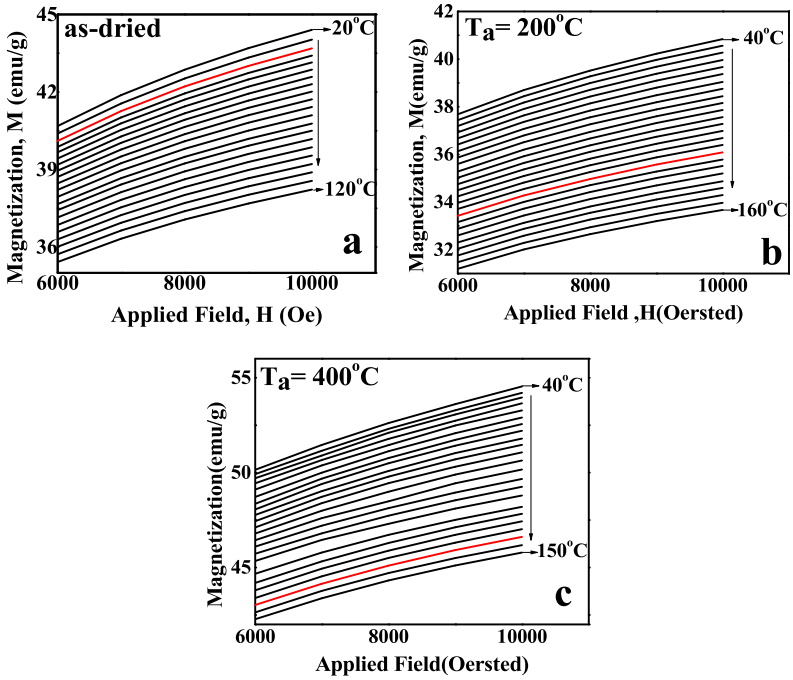

FIG. 6. (a) Isothermal magnetization curves for as-dried samples around Blocking temperature T_B. The red curve is the data for T_B. (b) Isothermal magnetization curves for T_a= 200°C around Blocking temperature T_B. The red curve is the data for T_B. (c) Isothermal magnetization curves for T_a= 400°C around Blocking temperature T_B. The red curve is the data for T_B.

Magnetocaloric effect (MCE) is the heating and cooling of a magnetic material due to the application of magnetic field. In order to explain the origin of magnetocaloric effect, thermodynamics is used which relates the magnetic variables (magnetization and magnetic field) to entropy and temperature. The physical origin of the MCE is the coupling of the magnetic sublattice to the applied magnetic field H, which changes the magnetic contribution to the entropy of the solid. The term MCE usually designates the much stronger effect, observed when a phase transition in the materials involves.[33,34] The transitions are identified as first or second order, structural or magnetic states of the material. In this regard, magnetic nanoparticles have distinctive advantages. Because, a flexible order-disorder transition associated with superparamagnetic blocked state referred to as the blocking transition (T_B) is revealed in nanoparticles.

In this study, MCE of $CoFe_2O_4$ nanoparticle was measured nearly blocking temperature for the as-dried sample and the samples annealed at 200°C and 400°C. To measure MCE, the calculation of change in entropy ΔS (T, ΔH) was carried out. To evaluate the MCE of the samples, the isothermal magnetization curves were collected at different fixed temperatures (Fig. 6). The measurement of $\partial M/\partial T$ was determined with change of magnetic field. The magnetic entropy change was determined by using the numerical integration called Maxwell's thermodynamic relation.[35–38]

$$\left(\frac{\partial S}{\partial H}\right)_T = \left(\frac{\partial M}{\partial T}\right)_H \tag{3}$$

Integrating over the field,

$$\Delta S = \int_0^H \left(\frac{\partial M}{\partial T}\right)_H dH \tag{4}$$

The trend of noticeable entropy change was tried to observe here. Typical values of the entropy change range in 0.1 to 1.0 J/kg/°C over the field of 1T for all the specimens. The temperature dependent entropy change ΔS for as-dried and samples at different annealing conditioned were shown in the Fig. 7. It is distinguishable that, ΔS increases uniformly with the increase of temperature for all specimens. In case of as-dried samples, there is no exhibition of following the shape of blocking peak

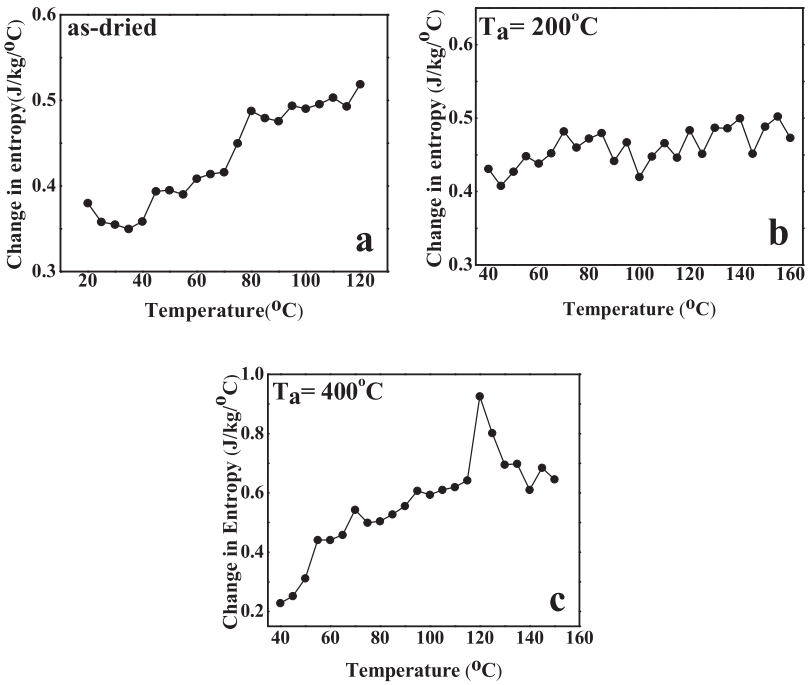

FIG. 7. (a) Entropy change vs Temperature curves for as-dried samples. (b) Entropy change vs Temperature curves for T_a= 200°C. (c) Entropy change vs Temperature curves for T_a= 400°C.

that is centered around 30°C. Measurement of isothermal curves at much lower temperature might be the layout of the scope of finding expected peak for this as-dried sample. For the samples annealed at 200°C, similar trend of entropy change is visible. There is no noticeable broad peak on or near T_B = 130°C. For the samples annealed at 400°C, a peak of maximum entropy change with the value of 0.93J/kg/°C can be observed at 120°C although T_B of the sample centered around 140°C.

IV. CONCLUSION

The structural, magnetic and magnetocaloric effect at various annealing conditions is studied here for Cobalt ferrite nanoparticles synthesized by Chemical co-precipitation method. The XRD study confirmed the formation of the single phase cubic spinel structure and the particle size are 5-10nm at different annealing temperature. Hysteresis loops demonstrates that the materials are in ferrimagnetic state which is in excellent agreement sextet pattern of Mössbauer spectra. The annealing operation causes an increase in saturation magnetization, remanent ratio, coercivity and superparamagnetic blocking temperature. Cation distribution and subsequent annealing operation contribute to these significant effects on magnetic properties. The magnetic entropy change (ΔS) of all specimens is showed around their respective blocking temperatures T_B. The trend of increasing ΔS as a function of temperature was observed for as-dried samples and T_a= 200°C and 400°C. Moreover, ΔS does not follow the shape of blocking peak which are centered at 30°C, 120°C and 140°C respectively.

ACKNOWLEDGMENTS

Materials Science Division, Atomic Energy Center, Dhaka, and Laboratory facilities of Centre for Advanced Research in Science (CARS), University of Dhaka are greatly acknowledged. Also the support of Ministry of Science and Technology, Bangladesh and International Science Program, Uppsala University, Sweden are acknowledged with gratitude.

[1] S. Singhal, T. Namgyal, S. Bansal, and K. Chandra, J. Electromagnetic Analysis & Applications **2**, 376–381 (2010).
[2] K. Maaz, A. Mumtaz, S. K. Hasanain, and A. Ceylan, J. Magn. Magn. Mater **308**(2), 289–295 (2007).
[3] A. Yakubu, Z. Abbas, N. A. Ibrahim, and M. Hashim, Phys. Sci. Int. Journal **8**(1), 1–8 (2015).
[4] C. Vázquez-Vázquez, M. Lovelle, C. Mateo, M. A. López-Quintela, M. C. Bujánnúñez, D. Serantes, D. Baldomir, and J. Rivas, Phys. Stat. Sol. (A) **205**(6), 1358–1362 (2008).
[5] B. Antic, M. Perovic, A. Kremenovic, J. Blanusa, V. Spasojevic, P. Vulic, L. Bessais, and E. S. Bozin, J. Phys.: Condens. Matter **25**, 1–13 (2013).
[6] M. Knobel, W. C. Nunes, L. M. Socolovsky, E. De Biasi, J. M. Vargas, and J. C. Denardin, J. of Nanosicence and Nanotechnology **8**, 2836–2857 (2008).
[7] J. Giri, P. Pradhan, V. Somani, H. Chelawat, S. Chhatre, R. Banarjee, and D. Bahadur, J. Magn. Magn. Mater **320**(5), 724–730 (2008).
[8] N. Sanpo, C. C. Berndt, C. Wen, and J. Wang, Acta Biometarialia **9**, 5830–5837 (2013).
[9] K. Hanium Maria, S. Choudhury, and M. Abdul Hakim, Int. Nano Lett. **3**(42), 1–10 (2013).
[10] S. Xavier, S. Thankachan, B. P. Jacob, and E. M. Mohammed, Nanosystems: Physics, Chemistry and Mathematics **4**(3), 430–437 (2013).
[11] N. Spaldin, *Magnetic materials: Fundamental and Device Applications* (Cambridge Univ Press, 2003).
[12] I. Sharifi, H. Shokrollahi, M. M. Doroodmand, and R. Safi, J. of Mag. and Mag. Materials **324**, 1854–1861 (2012).
[13] G. C. Papaefthymiou, S. R. Ahmed, and P. Kofinas, Rev. Adv. Mater. Sci. **10**, 306–313 (2005).
[14] A. Tishin and Y. Spichkin, *The Magnetocaloric Effect and Its Applications* (CRC Press, 2016).
[15] V. Pecharsky and K. Gschneidner, J. of Mag. and Mag. Materials **200**(1), 44–56 (1999).
[16] D. Jiles, *Introduction to magnetism and Magnetic Materials*, First ed., London, Chapman & Hall (1991).
[17] S. Manjura Hoque, Md. Sazzad Hossain, S. Choudhury, S. Akhter, and F. Hyder, Materials Letters **162**, 60–63 (2016).
[18] S. Choudhury, M. Alam Bhuiyan, and S. Manjura Hoque, Int. Nano Lett. **1**(2), 111–116 (2011).
[19] Md. Sazzad Hossain, S. Manjura Hoque, S. I. Liba, and S. Choudhury, AIP Advances **7**(10), 105321 (2017).
[20] M. Vucinic-Vasic, E. S. Bozin, L. Bessais, G. Stojanovic, U. Kozmidis-Luburic, M. Abeykoon, B. Jancar, A. Meden, A. Kremenovic, and B. Antic, J. Phys. Chem. C **117**, 12358−12365 (2013).
[21] K. Nadeem, S. Rahman, and M. Mumtaz, Progress in Natural Science: Materials International **25**(2), 111–116 (2015).
[22] E. F. Chagas, A. S. Ponce, R. J. Prado, G. M. Silva, J. Bettini, and E. Baggio-Saitovitch, J. Applied Physics **116**(3), 033901 (2014).
[23] P. Sharma and A. Sharma, Int. J. Material Sci & Engineering **4**(4), 208–214 (2016).
[24] K. Uestuener, M. Katter, and W. Rodewald, IEEE Transactions on Magnetics **42**(10), 2897–2899 (2006).
[25] S. R. Ahmed, S. B. Ogale, G. C. Papaefthymiou, R. Ramesh, and P. Kofimas, Appl. Phys. Lett. **80**(9), 1616–1618 (2002).
[26] R. S. Puche, M. J. T. Fernandez, V. B. Gutierrez, R. Gomez, V. Marquina, M. L. Marquina, J. L. P. Mazariego, and R. Ridaura, Bol. Soc. Esp. Ceram. **47**(3), 133–137 (2008).
[27] P. P. Vaishanva, U. Senaratne, E. Buc, and R. Naik, J. of App. Phy. **99**, 08G720 (2006).

[28] S. Manjura Hoque, S. I. Liba, A. Anirban, S. Choudhury, and S. Akhter, AIP Advances **6**(2), 025304 (2016).
[29] S. Manjura Hoque, M. Tariq, S. I. Liba, F. Salehin, Z. H. Mahmood, M. N. I. Khan, K. Chattopadhayay, R. Islam, and S. Akhter, Nanotechnology **27**(28), 285702 (2016).
[30] L. Ajroudi, N. Mliki, L. Bessais, V. Madigou, and S. Villain, Materials Research Bulletin **59**, 49–58 (2014).
[31] G. Bahmanrokh, M. Hashim, I. Ismail, N. Soltani, P. Vaziri, M. S. E. P. Shafie, and M. Navaseri, J. of Superconductivity and Novel Magnetism **26**(2), 407–414 (2013).
[32] X.-M. Lin and C. S. S. Anna, J. of Mag. and Mag. Materials **305**(1), 100–109 (2006).
[33] A. M. Tishin, Handbook of Magnetic Materials **12**, 395–524 (1999).
[34] V. K. Pecharsky and K. A. Gschneidner, J. of Mag. and Mag. Materials **200**(1), 44–56 (1999).
[35] S. Akhter, D. Paul, S. Hoque, M. Hakim, M. Hudl, and R. Mathieu, J. of Mag. and Mag. Materials **367**, 75–80 (2014).
[36] S. Hariharan and J. Gass, Rev. Adv. Mtr. Sci. **10**(5), 398–402 (2005).
[37] A. H. Morrish, *The Physical Principles of Magnetism* **74**, Wiley, New York (1965).
[38] M. H. Phan, M. B. Morales, C. N. Chinnasamy, B. Latha, and V. G. Harris, J. of Physics D: Applied Physics **42**, 2115007 (2009).